

Modal Analysis of a Heliostat for Concentrating Solar Power

D. Todd Griffith¹, Cliff K. Ho², Patrick S. Hunter³, Jeremy Sment², Adam C. Moya², and Anthony R. Menicucci²

Sandia National Laboratories⁴
Albuquerque, New Mexico 87185

ABSTRACT

A heliostat is a structure whose function is to reflect sunlight to a target collector. Heliostat vibrations can degrade optical pointing accuracy and fatigue the structural components. This paper reports on an experimental and analytical program with a goal to improve understanding of the response to wind loading on heliostats. A modal test was performed on a heliostat located at the National Solar Thermal Testing Facility (NSTTF) at Sandia Labs in Albuquerque, New Mexico. Modal tests were performed with artificial and natural wind excitation. Strain and displacements were also measured under wind loading. The information gained from these tests has been used to evaluate and improve structural models that predict the deformations of the heliostat due to gravitational and dynamic wind loadings. The paper will provide an up-to-date summary of model validation work, evaluation of suitable sensors, and development of data-processing methods for long-term deformation monitoring.

I. Introduction

A heliostat located at the National Solar Thermal Testing Facility (NSTTF) at Sandia Labs in Albuquerque, New Mexico, has been modal tested for validation of structural models and measurement of damping, strain and displacement under wind loading. This paper provides an up-to-date summary of the research effort [1]. The information gained from these tests will be used to evaluate and improve structural models that predict the motions/deformations of the heliostat due to gravitational and dynamic wind loadings. These deformations can cause optical errors and motions that degrade the performance of the heliostat. The main contributions of this work include: (1) a determination of the important dynamics of the heliostat structure as they relate to durability and optical accuracy, (2) evaluation design codes and models, and (3) evaluation of sensors and data-processing methods for long-term monitoring of heliostat deformations.

A goal of this work is to improve understanding of the effect of gravity and windy conditions on the optical accuracy of heliostats. Gravitational loads on the heliostat are static (constant) loads that cause the heliostat to deform under its own weight. Although the deformations may be small for a particular design, they may result in significant optical pointing errors as a result of the translation and rotation of the reflectors. The effect of gravity on optical errors can be reduced through an initial alignment of the facets. However, improved structural design using accurate, predictive structural models for the heliostat could reduce the time and costs associated with the alignment process that must be performed on thousands of nominally identical heliostats in a single field. In addition to constant gravitational loads, dynamic loads such as windy conditions and ground vibration can also result in optical errors. The effects of dynamic loading from windy conditions are the focus of the present work, and initial findings of this research program are presented in this paper. The effects of gravitational loads have been the focus of other works [2,3].

The National Solar Thermal Testing Facility (NSTTF), located at Sandia Labs in Albuquerque, New Mexico, contains a number of test facilities and commercial prototypes of various concepts for concentrating solar power systems. The focus of this work is on heliostats which operate at the Sandia National Laboratories' 5-MWt Central Receiver Test Facility (CRTF), as shown in Figure 1 with approximately 220 heliostats.

¹ Wind and Water Power Technologies Department

² Concentrating Solar Power Department

³ Engineering Sciences Center

⁴ Sandia National Laboratories is a multi-program laboratory managed and operated by Sandia Corporation, a wholly owned subsidiary of Lockheed Martin Corporation, for the U.S. Department of Energy's National Nuclear Security Administration under contract DE-AC04-94AL85000.



Figure 1. Aerial View of Sandia 5-MWt Central Receiver Test Facility

Significant vibrations, especially of the reflectors, can occur during windy conditions. The size of the vibrations depends on a variety of factors which include most notably the wind speed, wind gusts, size of the heliostat, and orientation of the facets with respect to the wind direction. One reference that addresses wind loading effects on heliostats is Reference 4. At very high wind speeds, the heliostat cannot be operated and must be stowed to avoid large wind loadings. However, at lower wind speeds it is desired to operate the heliostat with minimized optical errors due to the wind induced vibration. The present work seeks to improve the design and operation of heliostats by improving their performance during wind loading. The hope is that these tests will reveal important new information on the characterization of heliostat dynamics as well as methods for characterizing heliostat dynamics to support new design concepts in the concentrating solar power industry. Further, a natural question is in understanding which modes of vibration most strongly affect pointing accuracy and to what extent these modes are excited by the wind loading. The answer to these questions can guide future heliostat design decisions, particularly in optimizing the designs with respect to both structural loads and cost.

Building upon the prior work published in Reference 1, the current paper addresses in more detail measurements recorded under wind loading and planning for a field monitoring campaign. In particular, a summary showing the effect of wind speed on damping estimates is presented. The paper begins with a description of the test article and summaries of the preliminary finite element model prediction and the initial modal test design (Section II). In Section III, post-test model correlation and refinement are discussed. In Section IV, damping estimates for the wind loading cases are described as determined using an output-only modal analysis approach. These damping estimates are compared with damping for hammer excitation in calm winds. Also, dynamic strain measurements under wind loading are discussed. In Section V, a field instrumentation plan designed for long-term monitoring of the heliostat field is described along with plans for data processing methods. The paper concludes with a summary of current and future work.

II. Description of the test article and preliminary modal tests

A photo of the test heliostat is shown in Figure 2. The primary substructure is a “U” shaped structure called the yoke. The yoke sits upon an azimuth motor drive, which is fixed to the ground. The two uprights of the yoke are “I-beam” construction while the horizontal lower section of the yoke is a closed section. Atop the yoke, connected at the top of both uprights of the yoke, is the torque tube. The torque tube is a continuous member with annular cross-section. The torque tube rests on the yoke with the elevation drive located at the top of one upright of the yoke while a roller bearing is located at the top of the other upright. Truss structures, which support the facets (reflectors), are cantilevered from the torque tube. As can be seen from Figure 2, the facets are supported by a pair of trusses (one long truss and one short truss). A total of five columns of facets are along the length of the torque tube extending in opposite directions. The columns of facets are independent as neither the trusses nor the facets of one column are connected to a different column. The major structural elements are comprised of steel with the exception of the facets which are comprised of two panes of glass with reflecting material in between. The heliostat pointing direction is controlled through the azimuth and elevation drives. A number of heliostat configurations are possible when considering the stowage configuration through the full range of operating configurations.



Figure 2. Description of Heliostat Major Structural Elements

A pretest finite element model was developed using SolidWorks®. The initial model of the heliostat structure included the detailed geometry of the major structural elements. The mesh for the heliostat consisted of approximately 6,000,000 nodes and 3,000,000 elements with an element size of 0.92 in. The mesh was completely comprised of solid 3D tetrahedral elements. The numerical solution used is an iterative solver called FFEPlus which is more efficient when solving models with a large number of DOF's.

The joints in the structure (namely the azimuth drive, elevation drive, and bearing) were modeled as rigid elements. Initially, this is a reasonable assumption. However, it is common to learn during a modal test that modes exist that are associated with motion ("slop") in the joints. We term these modes as rigid body modes throughout the paper. The preliminary modal analysis is presented here. This pretest analysis is very important to support the modal test design as it can be utilized to determine the necessary sensor characteristics as well as aid in placement of the sensors to measure a desired set of modes of vibration.

A few of the predicted shapes for the modes of vibration with the facets oriented vertically are plotted in Figure 3 (a through d). These modes are the 4 lowest frequency modes predicted in the pretest finite element analysis for this configuration. The first ten modes have predicted natural frequency of 1.60 to 4.08 Hz.

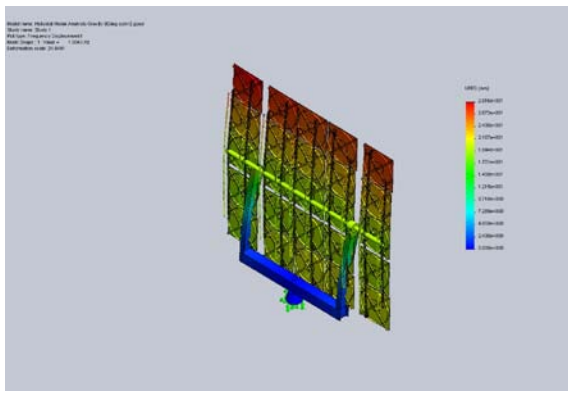


Figure 3(a). Yoke Bending In-plane

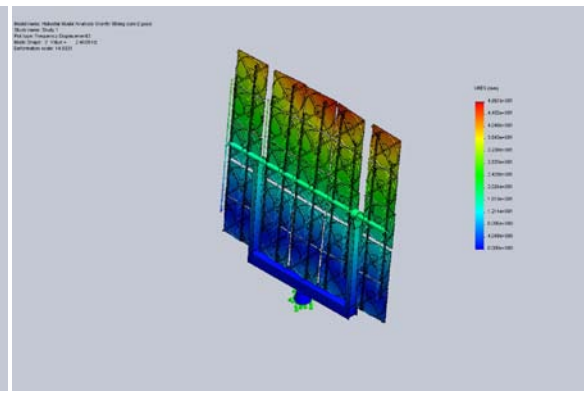


Figure 3(b). Yoke Bending Out-of-plane

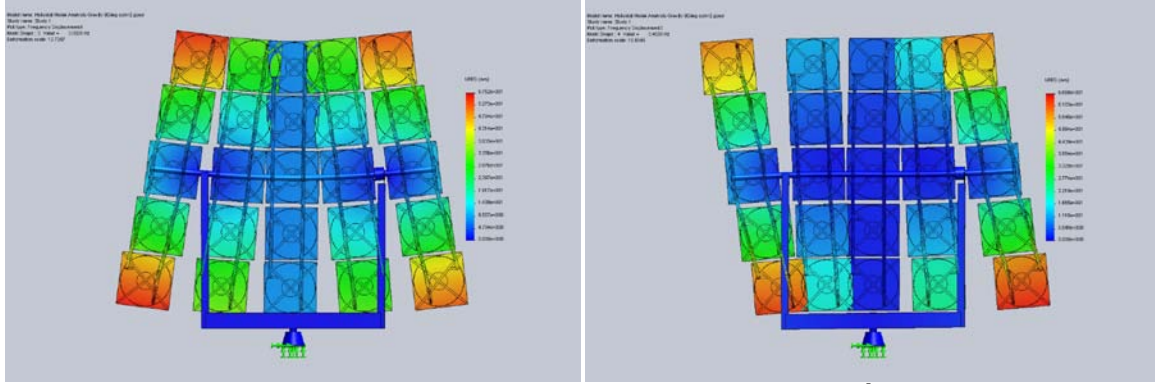


Figure 3(c). 1st Torque Tube Bending

Figure 3(d). 2nd Torque Tube Bending

Figure 3. Four Lowest Frequency Pretest Analysis Mode Shapes for Vertical Configuration

Figure 3(a) shows the lowest frequency predicted mode, which is bending of the yoke in the in-plane direction. This confirms intuition because the in-plane direction is the “soft” direction of the I-beam yoke uprights. Figure 3(b) shows bending of the yoke in the out-of-plane direction, which is the “stiff” direction of the uprights. Figure 3(c) shows a fundamental bending mode of the torque tube. As can be seen, the columns of the heliostat rotate with small deformation of the trusses. Figure 3(d) shows a more complex bending mode of the torque tube. The fifth mode is similar to the second mode; however, the two uprights are moving out-of-phase. Starting with the sixth mode, significant in-plane bending of the trusses is predicted with small motions of the yoke and torque tube.

These predictions show that the lowest frequency modes of vibration involve bending of the yoke, bending of the torque tube, and in-plane bending of the truss/facet structures. At higher frequency out-of-plane bending of the truss/facet structures are present. Based on intuition, we expect that rigid body modes of the system will exist at relatively low frequency (at least in the range of these pretest predicted modes) for the azimuth and elevation drive rotational degrees of freedom. Therefore, in addition to measuring the above target modes in the modal test, we also designed the test instrumentation to investigate additional modes such as the rigid body modes. This is important because rigid body modes may have significant sized motions due to wind loading and may need to be included in the model.

The test was designed so that modal test could be conducted for a range of elevation angles. Figure 4 shows a plot demonstrating the three test configurations with 0 degree (vertical), 45 degree, and 90 degree (reflectors down) orientations.

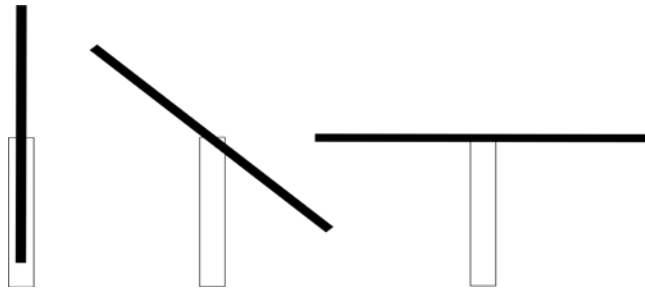


Figure 4. Test Configurations: 0 Degrees, 45 Degrees, and 90 Degrees (from left to right)

Figure 5 shows the instrumentation layout. Each symbol in the figure indicates a location in which a sensor was mounted. The locations for these sensors were chosen based on the pretest finite element analysis (Figure 3). This instrumentation plan was expected to provide measurement of the first 10 predicted modes as well as rigid body modes and higher frequency out-of-plane truss bending modes. The blocks indicate triaxial accelerometers. Triaxial accelerometers were chosen so that all of the test configurations shown in Figure 4 could be tested without the need for moving or re-orienting sensors. Triaxial accelerometers with sensitivities of 100, 500, and 1000 mV/g were mounted at the ends of the trusses for evaluation. It was found that 100 mV/g accelerometers did not provide sufficient sensitivity for low wind speeds, while 500 and 1000 mV/g did. It was found that the best option were the 1000 mV/g sensors because they were not over-ranged even for 30+ mph winds. Figure 6(a) shows a truss mounted accelerometer with magnetic mount.

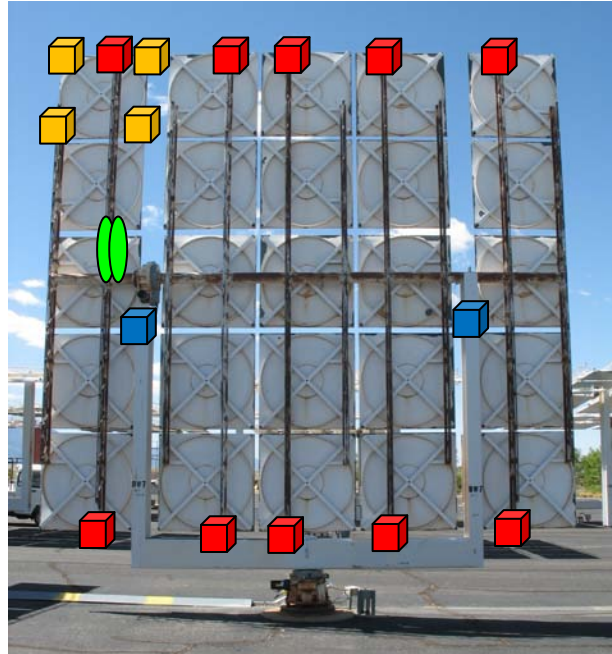


Figure 5. Instrumentation Layout for Preliminary Modal Test

The green ovals in Figure 5 indicate strain sensors. High-output, dynamic, piezoelectric strain sensors were used. It was decided for the initial testing to mount two gauges on a single truss for evaluation. The sensors were positioned such that one measured primarily in-plane truss bending strain while the other measured primarily out-of-plane truss bending strain. Figure 6(b) shows a close-up of the two mounted strain sensors, which were glued to the surface once it had been sanded to a smooth finish.



Figure 6(a). Truss Mounted Accelerometer

Figure 6(b). Piezoelectric Strain Sensors

Multiple excitation methods were considered including both artificial and natural excitation. For hammer tests, it is, of course, important that all inputs be quantified. Therefore, during hammer impact tests it was desired that wind speeds be very low or calm during data acquisition. Of course no control can be placed on the weather during field testing; therefore, we chose to record impact hammer data during calm periods and wind-excited data during windy conditions. Fortunately, suitable windows of opportunity for both types of data collection were possible during the scheduled testing period. In order to reduce the effect of even very low winds during impact testing, a sufficient number of averaged measurements were recorded to minimize the noise effect of the random wind input.

Figure 7 shows a broad view of the test setup. To the left is the anemometer for measuring wind speed and direction. The height of the anemometer was just above the torque tube height and located about 50 feet from the test heliostat. The test

heliostat was located along the perimeter of the field. As a result, the anemometer was able to provide a simple measurement of the free-stream inflow conditions.

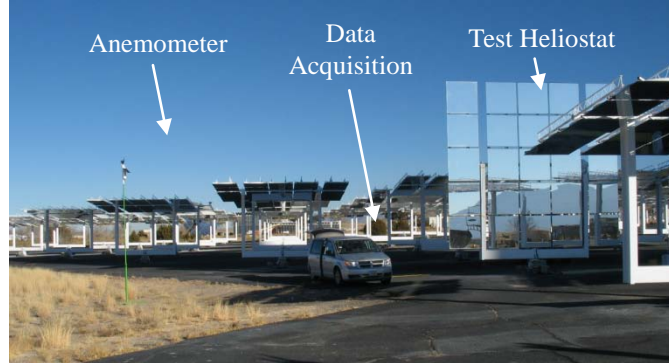


Figure 7. Test Setup with Wind Speed Measurement

Wind excitation was performed for both low winds (5-10 mph) as well as high wind (10-30 mph). Wind speed and direction measurements were recorded during all of the tests at a few locations about the perimeter of the heliostat field. These tests were also performed with the heliostat in multiple configurations. The 0, 45, and 90 degree configuration were tested with the heliostat facing south (into the wind) as well as facing east (edge one to the wind). The analysis of this data should provide a good indication of the coupling between the wind and the modes of vibration. Autospectrum and time histories were recorded for a total of 68 minutes. The data was binned so that 100 overlapping averages were performed in calculating the autospectrum. Furthermore, the hammer impact tests were performed for wind speeds below 5 mph. Therefore, the effect of wind speed on the modal parameters (in particular the damping) can be determined for 3 ranges of wind speeds.

III. Model Correlation and Calibration

The Sandia SMAC code was used to extract the modal parameters from FRFs measured during hammer tests [5]. Table 1 lists the measured natural frequencies for the 0 degree configuration and compares with the pretest predicted frequencies. The in-plane yoke bending mode and the first and second torque tube bending modes have very good agreement. However, the two out-of-plane yoke bending modes (modes 2 and 5 in Table 1) show a large discrepancy. Based on analysis of multiple data sets and viewing of experimental mode shapes it is believed that these two modes are either coupled to the rigid body mode associated with the elevation drive or depend strongly on the stiffness of the elevation drive joint, which was modeled as rigid in the pretest analysis. The initial model correlation indicated that the model requires modifications for the out-of-plane yoke bending behavior. In addition, the out-of-plane yoke bending modes depend the most on the configuration (elevation angle) of the heliostat, likely due to the effect of the changing inertia of mirror structures. Mode 6 was not observed in the 0 degree test data. This mode is very similar to modes 7 and 8, and it is possible this mode was not well-excited or could not be identified by the system identification algorithm as it is a closely spaced mode. However this mode, whose behavior is weakly dependent on orientation, was identified in the 45 and 90 degree orientation tests. The in-plane bending mode predictions (modes #7 through #10) are in reasonably good agreement (about 10%). Due to the symmetry and repeated structures of the heliostat columns, closely spaced mode families are present. For example, modes 6 through 8 are a family of in-plane bending modes with similar mode shapes but having different phasing of the column motions. Likewise, modes 9 and 10 belong to a family of modes having similar mode shapes. Although not listed, a rigid body mode of the azimuth drive was measured at 1.28 Hz. Each of the modes listed in Table 1 were found to have very small measured damping of 0.1 to 0.25% of critical damping.

Table 1. Natural Frequency Comparison: 0 Degree Configuration

Mode No.	Mode Description	Pretest Predicted Frequency(Hz)	Modal Test, Impact Hammer Frequency (Hz)
1	Yoke Bending (in-plane)	1.604	1.63
2	Yoke Bending (out-of-plane)	2.465	1.98
3	1 st Torque Tube Bending	3.002	3.03
4	2 nd Torque Tube Bending	3.453	3.57
5	Yoke Bending (out-of-plane, out-of-phase)	3.787	2.42
6	In-plane Bending (1)	3.847	--
7	In-plane Bending (2)	3.879	4.21
8	In-plane Bending (3)	3.923	4.37
9	In-plane (truss bending, 1)	4.075	4.60
10	In-plane (truss bending, 2)	4.080	4.64

Current work is focusing on improvements to the structural model. Calibration of stiffness in the “joints” associated with the azimuth drive (at the base of the heliostat) and the elevation drive and roller joint is being pursued. These three joints are being modeled using linear and rotation spring degrees of freedom using Sandia’s SALINAS Structural Dynamics Code [6]. Early results indicate that modeling these joints with springs as opposed to the pre-test rigid connections can improve predictions for both yoke out-of-plane bending modes as well as inclusion of the azimuth and elevation rigid body modes.

IV. Analysis of Wind Excited Data

A special version of the SMAC algorithm [5] was used to identify the modal parameters from the wind-excited response measurements. SMAC uses cross-spectrum functions, which were post-processed from time history measurements. The identified frequencies were in very close agreement with those from the hammer-excited tests. However, the damping was significantly higher for the wind-excited tests. For the hammer tests, wind speeds were calm or very low; therefore, the damping estimates only include the inherent structural damping mechanism. For the wind-excited tests, the measured damping was higher and included both the structural damping as well as aerodynamic damping from the wind.

Table 2 shows the extracting damping values for a few of the modes that were identified using the special OMA version of the SMAC code. Damping is shown for two wind speed magnitudes: (1) zero or calm (hammer tests) and (2) high winds at 10-30 mph (wind excited). It was expected that the aerodynamic component of damping is proportional to wind speed, and these measurements confirm this intuition. The results show that damping increases in the range from 24 to 120% for this set of in-plane bending modes at higher wind speeds. Although not tabulated, analysis of damping for modes with out-of-plane motion shows even larger increases of 200% or more. The modes of vibration of this heliostat are very lightly damped even with aerodynamic damping.

Table 2. Damping Values with Wind Speed Magnitude (0 degree configuration)

Mode No.	Mode Description	Pretest Predicted Frequency(Hz)	Damping (%) Very low wind	Damping (%) 10-30 mph
1	Yoke Bending (in-plane)	1.604	0.235	0.299
3	1 st Torque Tube Bending	3.002	0.117	0.228
4	2 nd Torque Tube Bending	3.453	0.183	0.402
7	In-plane Bending (2)	3.879	0.257	0.319

Strain measurements also indicated the suitability of dynamic strain gauges for this test application. These sensors performed extremely well with excellent low noise characteristics. Strain time histories were recorded which demonstrated a relation with the wind speed, and which demonstrated large response at the modal frequencies. The performance of these gauges for strain measurement due to dynamic loads is superior to traditional strain sensors as the sensitivity is much higher permitting meaningful measurement of strain for even very low wind speeds. Although the sensitivity of these strain sensors

is high, a well-known difficulty in using strain gauges is lack of certainty in measurement sensitivity with the glued mount. Determination of frequency and damping information is possible with very good accuracy; however, determination of mode shapes or estimation of strain or displacement amplitude has greater uncertainty.

V. The Field Monitoring Campaign

The initial modal tests and analysis work was conducted in support of a field monitoring campaign that is currently being implemented. The modal tests provided a means to improve the structural design models, to identify important dynamic behavior that is excited by the wind loads, and to select sensors that are suitable for field monitoring implementation as well as data processing requirements. A concept for the field monitoring campaign is shown in Figure 8. Interior units are likely to experience a much different wind loading than the units on the perimeter [4] due to blocking and wake effects. Therefore, careful attention is being placed on selection of units for long-term monitoring.

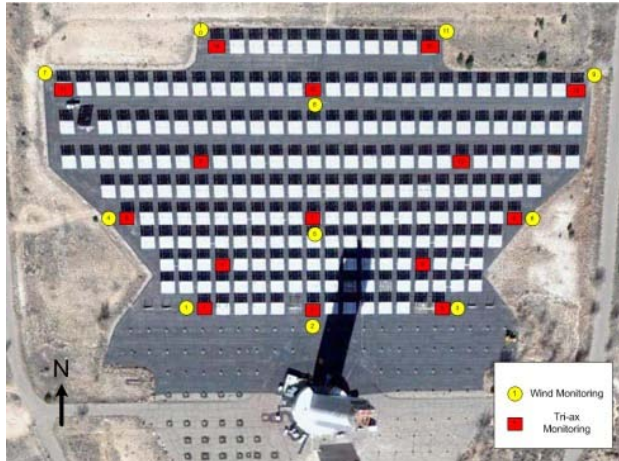


Figure 8. Concept for Monitoring of Heliostat Field

This monitoring plan will include the use of accelerometers, strain sensors, and anemometers. Both DC and traditional piezoelectric type accelerometers will be used. Piezoelectric strain gauges like those used in the initial modal tests will be deployed. Anemometers will also be used to record wind speed and direction along with the acceleration and strain measurements. The system will include over 200 channels of acquisition.

The measurements will be processed to evaluate continuous monitoring of heliostat systems. One focus will be on characterizing performance during high wind speed conditions in which the heliostat is operating and below the critical stowage wind speed. A method is under development that can be used to estimate displacements from acceleration measurements. The hope is that this approach can be used to directly compute displacements at the sensor locations, and ultimately provide a means to estimate the full-field dynamic displacement field of the heliostat using modal filtering techniques. With full-field displacement estimates, the optical accuracy of the heliostat could be quantified using a few heliostat mounted sensors. A key focus will be placed on developing a better understanding of various wind loading effects including quasi-static loading response, gust response, and vortex induced vibration, which span a frequency range from near DC to about 20 Hz. Another focus will be on durability assessment. Strain sensors will provide fatigue cycle counting on critical heliostat components. Accelerometer data will also be considered to estimate the size of motions in critical heliostat components.

The heliostat is a very good candidate for evaluation of OMA identification techniques for a number of reasons including: (1) the modes are well-excited with wind loading, (2) a number of closely spaced modes exist due to repeated structures, (3) the modes are lightly damped but also vary with wind speed and direction, (4) the configuration of the heliostat can be held stationary or operated at slow rotation rates (although many modes do not vary with orientation changes), and (5) hammer testing is feasible to provide a benchmark comparison set of modes for calm wind conditions. One observation of this work is the need for output-only identification of a larger number of modes with improved automation. An automated method extracting the modal parameters during the field instrumentation campaign could be very valuable. It is our hope to utilize these data sets to evaluate OMA techniques.

VI. Conclusions and Future Work

Field modal tests and finite element analysis were performed to study the modes of vibration of a heliostat located at the Sandia Central Receiver Test Facility. The modal behavior of the heliostat can be described as low-frequency, lightly damped

and strongly wind-excited. A number of closely spaced modes were present along with rigid body modes associated with the drive mechanisms.

Initial model correlation indicated that springs were needed in the models not only to permit rigid body motion in the drive mechanisms but also to aid in improving the correlation of out-of-plane yoke bending modes which had initially large discrepancy. The tests demonstrated that rigid body modes associated with motion about the azimuth and elevation drives should be included in the model as these were found to be relatively low frequency modes that may be excited by the wind and contribute to degradation of optical accuracy. Current modeling efforts show promise to both include the rigid body motion and reconcile the out-of-plane yoke bending modes. It should be noted that although a few modes were in poor agreement, the pre-test models showed very good agreement for most of the modes including in-plane and out-of-plane truss bending modes and torque tube bending modes.

OMA identification was used to estimate damping for wind-excited tests. When compared to hammer data with calm winds, the increase in damping due to aerodynamics was demonstrated. The field monitoring campaign that is currently underway will seek to perform additional work in evaluating OMA techniques for this application. In addition, methods are under development for estimation of displacement for use in quantifying optical accuracy. Another focus of the monitoring campaign is assessing durability of the heliostat components. The hope is that this work will aid in improving heliostat designs to mitigate wind loading effects on performance and durability. In addition, this work may provide insight on the deployment of sensors in a heliostat field for monitoring applications.

VII. Acknowledgments

The authors would like to thank a number of people from Sandia Labs who made significant contributions to the planning and execution of these tests. Cheryl Ghanbari helped in the early test planning and logistics and helped identify a suitable heliostat for these tests. Ron Briggs performed much of the pretest safety analysis. Ernie Trujillo provided significant support of sensor installation and operation of the heliostat and portable lift. Ron Coleman and David Smallwood suggested methods to produce displacements from acceleration measurements and performed preliminary laboratory assessments. Randy Mayes provided a special version of the SMAC code for OMA identification of the wind excited data sets.

Sandia National Laboratories is a multi-program laboratory managed and operated by Sandia Corporation, a wholly owned subsidiary of Lockheed Martin Corporation, for the U.S. Department of Energy's National Nuclear Security Administration under contract DE-AC04-94AL85000. The United States Government retains and the publisher, by accepting the article for publication, acknowledges that the United States Government retains a non-exclusive, paid-up, irrevocable, world-wide license to publish or reproduce the published form of this manuscript, or allow others to do so, for United States Government purposes.

References

- [1] Griffith, D.T., Moya, A., Ho, C., and Hunter, P., "Structural Dynamics Testing and Analysis for Design Evaluation and Monitoring of Heliostats," *Proceedings of the 5th ASME International Conference on Energy Sustainability*, August 7-10, 2011, Washington, DC, USA, ESFuelCell2011-54222.
- [2] Christian, J.M., Ho, C.K., "Finite Element Modeling of Concentrating Solar Collectors for Evaluation of Gravity Loads, Bending, and Optical Characterization," *Proceedings of the 4th ASME International Conference on Energy Sustainability*, May 17-22, 2010, Phoenix, Arizona, USA, ES2010-90050.
- [3] Moya, A.C., Ho, C.K., "Modeling and Validation of Heliostat Deformation Due to Static Loading," *Proceedings of 5th ASME International Conference on Energy Sustainability*, August 7-10, 2011, Washington, DC, USA, ESFuelCell2011-54216.
- [4] Peterka, J.A. and Derickson, R.G., "Wind Load Design Methods for Ground-based Heliostats and Parabolic Dish Collectors," Sandia National Laboratories Technical Report, SAND-92-7009, September 1992.
- [5] Mayes, Randall L. and Klenke, Scott E., "The SMAC Modal Parameter Extraction Package," *Proceedings of the 17th International Modal Analysis Conference*, pp. 812-818, February 1999.
- [6] Bhardwaj M., Reese, G., Driessen, B., Alvin, K., and Day, D., "SALINAS - An Implicit Finite Element Structural Dynamics Code Developed for Massively Parallel Platforms," *Proceedings of the 41st AIAA/ASME/ASCE/AHS/ASC Structures, Structural Dynamics, and Materials Conference*, April 3-6, 2000, Atlanta, GA, USA, AIAA 2000-1651.